ENVIRONMENTAL RESEARCH
LETTERS

LETTER • OPEN ACCESS

Influence of a Carrington-like event on the atmospheric chemistry, temperature and dynamics: revised

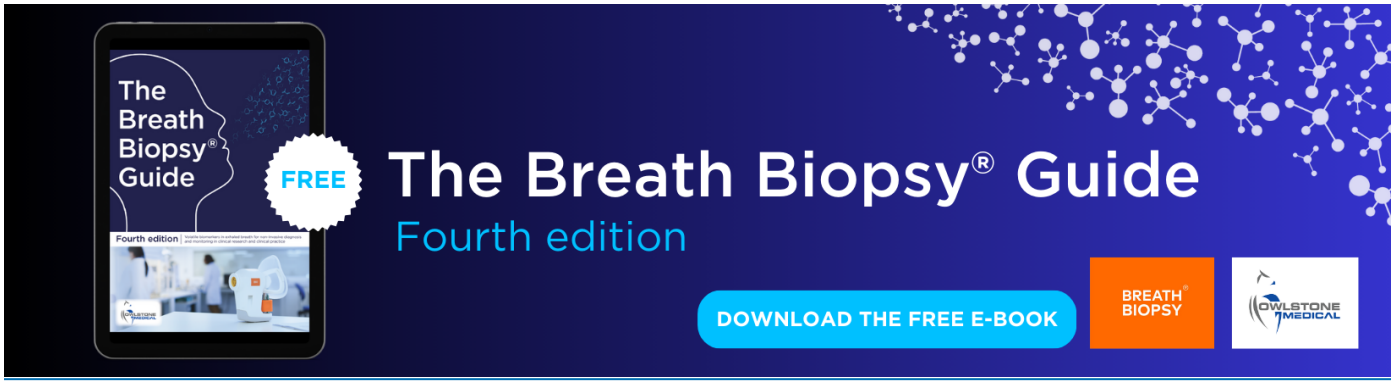

OPEN ACCESS
IOP PUBLISHING
ENVIRONMENTAL RESEARCH LETTERS
Environ. Res. Lett. **8** (2013) 045010 (10pp)
doi:10.1088/1748-9326/8/4/045010

Influence of a Carrington-like event on the atmospheric chemistry, temperature and dynamics: revised

M Calisto[1], I Usoskin[2] and E Rozanov[3,4]

[1] International Space Science Institute (ISSI), Bern, Switzerland
[2] Sodankylae Geophysical Observatory (Oulu unit) and Department of Physics, University of Oulu, FI-90014 Oulu, Finland
[3] Physical-Meteorological Observatory/World Radiation Center, Davos, Switzerland
[4] Institute for Atmospheric and Climate Science ETH, Zurich, Switzerland

E-mail: Marco.Calisto@issibern.ch

Received 25 June 2013
Accepted for publication 24 September 2013
Published 16 October 2013
Online at stacks.iop.org/ERL/8/045010

Abstract
This study investigates the influence of a major solar proton event (SPE) similar to the Carrington event of 1–2 September 1859 by means of the 3D chemistry climate model (CCM) SOCOL v2.0. Ionization rates were parameterized according to CRAC:CRII (Cosmic Ray-induced Atmospheric Cascade: Application for Cosmic Ray Induced Ionization), a detailed state-of-the-art model describing the effects of SPEs in the entire altitude range of the CCM from 0 to 80 km. This is the first study of the atmospheric effect of such an extreme event that considers all the effects of energetic particles, including the variability of galactic cosmic rays, in the entire atmosphere. We assumed two scenarios for the event, namely with a hard (as for the SPE of February 1956) and soft (as for the SPE of August 1972) spectrum of solar particles. We have placed such an event in the year 2020 in order to analyze the impact on a near future atmosphere. We find statistically significant effects on NO_x, HO_x, ozone, temperature and zonal wind. The results show an increase of NO_x of up to 80 ppb in the northern polar region and an increase of up to 70 ppb in the southern polar region. HO_x shows an increase of up to 4000%. Due to the NO_x and HO_x enhancements, ozone reduces by up to 60% in the mesosphere and by up to 20% in the stratosphere for several weeks after the event started. Total ozone shows a decrease of more than 20 DU in the northern hemisphere and up to 20 DU in the southern hemisphere. The model also identifies SPE induced statistically significant changes in the surface air temperature, with warming in the eastern part of Europe and Russia of up to 7 K for January.

Keywords: space weather, modeling, Carrington event

1. Introduction

Solar proton events (SPE) are sporadic events with enhanced flux of energetic particles (mostly protons) of solar origin observed at the Earth's orbit. They usually correspond to strong solar flares and/or coronal mass ejections (CME) when ions can be accelerated to high energies of up to a few GeV (Reames 1999). When entering the Earth's magnetic field, these energetic protons are mostly deflected. However, protons with sufficiently high kinetic energy can penetrate the atmosphere and cause massive ionization including production of HO_x ($H + OH + HO_2$) and NO_x ($NO + NO_2$) at the polar cap areas (Patterson *et al* 2001, Jackman *et al* 2009). These energetic particles guided by the magnetic field into the polar regions collide with the Earth's atmosphere transferring their kinetic energy into potential energy through the process of ionization, for example $X_2 + p \rightarrow X_2^+ + p + e^*$, producing fast secondary electrons ($X = N, O$ and the star symbolizes high kinetic energy). These electrons

can dissociate the nitrogen molecule, producing both, the electronic ground state and the electronic first excited state of the nitrogen atom. The latter reacts readily with O_2, producing nitric oxide, $N(^2D) + O_2 \rightarrow NO + O$.

Below the mesopause, where water cluster ions form, the ionization through the solar protons contributes also to the formation of HO_x radicals. For example, molecular oxygen ions (O_2^+) produced by an SPE form O_4^+ ions via attachment of molecular oxygen, which then react with water. This hydrated ion quickly hydrates further to produce OH via $O_2^+ \cdot H_2O + H_2O \rightarrow H_3O^+ \cdot OH + O_2 \rightarrow H_3O^+ + OH + O_2$.

The produced HO_x, however, has only a short lifetime of a few days, whereas NO_x can have a lifetime of weeks in which they can deplete atmospheric ozone (Solomon *et al* 1983, Reid *et al* 1991). This ozone depletion by the energetic protons has also been detected with satellite measurements (Randall *et al* 2001, Seppälä *et al* 2004, von Clarmann *et al* 2013). The impact of the energetic protons is best visible in the winter hemisphere, because at that time, the polar vortex is stable and the air within is trapped. Thus, the reactions happening within the vortex can take place without getting disturbed from outside air.

The topic of modeling the impact of the Carrington event on the Earth's atmosphere with a 3D chemistry climate model (CCM) has, to our knowledge, not been conducted extensively. Thomas *et al* (2007) was the first study using a 2D model investigating the Carrington event. Rodger *et al* (2008) have analyzed with their 1D model the effects of such an event on the Earth's atmosphere and Calisto *et al* (2012) used a 3D CCM for their analysis. These two papers have in common that they have adopted the same altitude dependent ionization rates (IR) to find out what the impact of the Carrington event on the atmosphere might be.

The previous model studies were inconsistent in two ways. First, they were based on truncated models of the atmospheric ionization incapable to deal with high energy (above a few hundred MeV) particles and thus unable to study tropospheric effects (see discussion in Bazilevskaya *et al* 2008). Moreover, the earlier studies did not take into account possible variations of the background ionization level due to GCR that is essential during geomagnetic storms, that is known as Forbush decreases, when the GCR intensity near Earth is reduced by an essential fraction (up to 25%) during several days or even weeks. A reduction of the atmospheric ionization due to this suppression of the GCR flux usually compensates or even over-compensates the enhanced ionization due to SEPs, leading to the net reduction of the atmospheric ionization, especially in the troposphere and low-middle stratosphere (Usoskin *et al* 2011). Since the Carrington event was accompanied by huge geomagnetic storms (Shea *et al* 2006), it expectedly led to a strong Forbush decrease and, thus, to a net reduction of the atmospheric ionization. Neglect of this may lead to erroneous results. Here we considered this effect in full detail.

Here we study, for the first time, the full effect of a strong SPE/geomagnetic event similar to the Carrington event. This approach is further motivated by Barnard *et al* (2011), who argue that the number of large SPEs will likely be enhanced throughout the next years. We use the recently developed CRAC:CRII (Cosmic Ray induced Cascade: Application for Cosmic Ray Induced Ionization) model for the atmospheric ionization, and then apply the event-based local model to force the global CCM SOCOL, focusing on the impact of CRII-induced NO_x and HO_x on chemistry, temperature and dynamics from the ground to 0.01 hPa barometric pressure (altitude of ~80 km).

We have also addressed the difference between the state-of-the-art parameterization of the improved ionization rate by Usoskin *et al* (2010) and the parameterization used in the papers by Rodger *et al* (2008) and Calisto *et al* (2012).

The models and experimental setup are described in section 2, the results containing the effects of the solar protons on several chemical species and the comparison between the parameterizations by Usoskin *et al* (2010) and the parameterization used in Rodger *et al* (2008) and Calisto *et al* (2012) are presented in section 3. In section 4 we give a short summary of the results.

2. Model description and experimental setup

For our experiment we have used the chemistry climate model SOCOL v2.0 (modeling tool for SOlar Climate Ozone Links) (Schraner *et al* 2008). The CCM SOCOL is a combination of the GCM MA-ECHAM4 and the chemistry transport model (CTM) MEZON. MA-ECHAM4 (Manzini *et al* 1997) is a spectral model with T30 horizontal truncation resulting in a grid spacing of about 3.75°; in the vertical direction the model has 39 levels in a hybrid sigma pressure coordinate system spanning the model atmosphere from the surface to 0.01 hPa; a semi-implicit time stepping scheme is used with a time step of 15 min in the dynamical core and physical process parameterizations; full radiative transfer calculations are performed every 2 h, but heating and cooling rates are calculated every 15 min.

The chemical-transport part MEZON (Rozanov *et al* 1999, Egorova *et al* 2003, 2005) has the same vertical and horizontal resolution as MA-ECHAM4, and the calculations are performed every 2 h. The model chemistry scheme treats 41 chemical species of the oxygen, hydrogen, nitrogen, carbon, chlorine and bromine groups, which are determined by gas-phase, photolysis and heterogeneous reactions in/on aqueous sulfuric acid aerosols, water ice and nitric acid trihydrate (NAT). Mixing ratios as a function of time of long lived well-mixed gases (e.g. N_2O, CH_4, ODS) were prescribed in the planetary boundary layer with no spatial dependency, while the fluxes of NO_x and CO were prescribed using emission data sets. The sea surface temperatures and sea ice distributions were prescribed from observational data.

In this letter we approximate the properties of a Carrington-like event by using the recently developed CRAC:CRII model (see Usoskin *et al* 2004, Usoskin and Kovaltsov 2006), which has been extended from the stratosphere (Usoskin and Kovaltsov 2006) to the upper atmosphere (Usoskin *et al* 2010). The model is based on a Monte Carlo simulation of the atmospheric cascade and reproduces the observed data within 10% accuracy in the

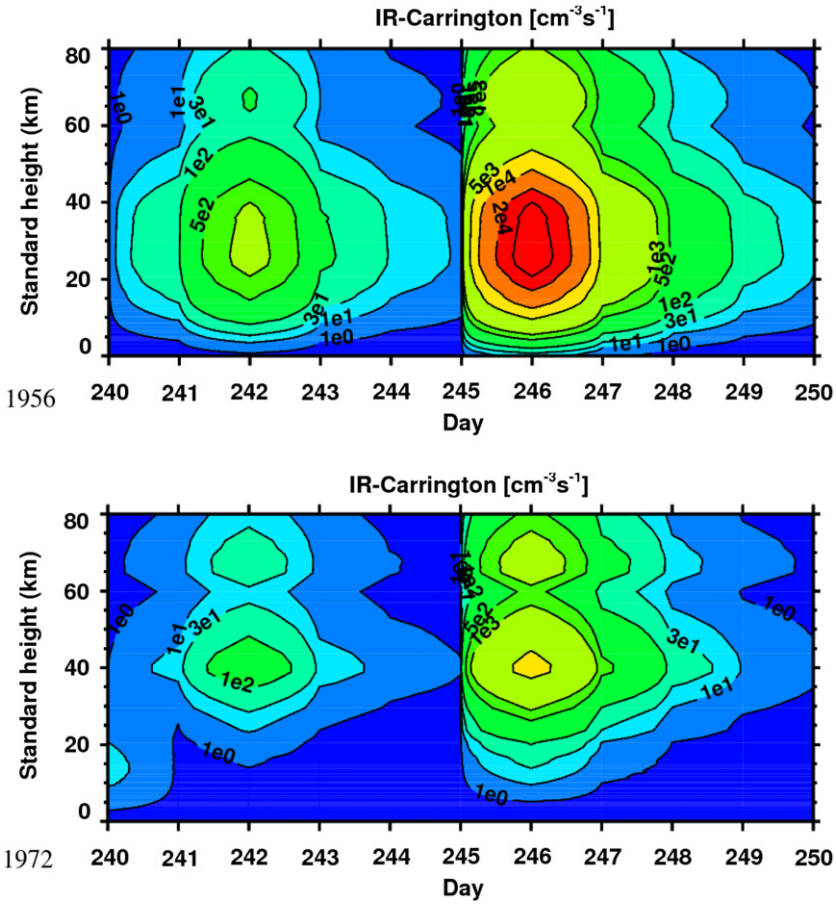

Figure 1. Height versus time evolution of ionization rates for the investigated solar proton event with the first impact at day 242 and the second impact at day 246. The upper panel shows the ionization from the 1956-type event, the lower panel from 1972, respectively. The data is given in ion pairs cm^{-3} s^{-1}.

troposphere and lower stratosphere (Bazilevskaya *et al* 2008, Usoskin *et al* 2009). The CRAC:CRII model has been verified by comparison with available direct data sets and other models (e.g., Bazilevskaya *et al* 2008, Usoskin *et al* 2009). It does, however, underestimate the ionization above ∼30 km since it neglects UV irradiance (UVI) and precipitating particles (higher up in the polar atmosphere). On the other hand, the parameterization used in the papers by Rodger *et al* (2008) and Calisto *et al* (2012) stops at 20 km which makes it difficult to determine full ionization in the whole atmosphere (see figure 1 for comparison of the IR).

Moreover, the earlier models neglected variability of the background ionization due to the GCR, which may be very important during strong geomagnetic disturbances (Usoskin *et al* 2011). Major geomagnetic disturbances are usually accompanied by Forbush decreases (FD) of GCR, caused by the same interplanetary transients (often a CME-driven shock wave). Although there is no clear general quantitative relation between the geomagnetic disturbance and the magnitude of a FD (Kane 2010), strongest geomagnetic storms ($Kp > 8$) are related to major FDs (magnitude >10%) (Belov *et al* 2001). Since the period of late August–early September 1859 was characterized by very strong geomagnetic disturbances (Humble 2006, Shea *et al* 2006) with two peaks: on DOYs 240 (telegraph disruptions and extended aurora—Humble 2006) and DOY 244–245 with Dst possibly reaching an extreme value of −1760 nT (Tsurutani *et al* 2003), we expect that at least two FDs would occur during that period leading to a strong suppression of the GCR flux. Although we cannot reconstruct exact magnitude and time profile of the FDs, we make a reasonable conservative assumption. We assume that both FDs were typical strong FDs with the magnitude of 15% for a polar NM, which is consistent with, e.g., the FD of August 1972. Second, we assume that the recovery time of GCR intensity was 4 days, which is typical for moderate-strong FDs (Usoskin *et al* 2008). We note that this is a conservative assumption as such an extreme geomagnetic storm may be accompanied by a larger FD.

The parameterization of the ionization rates cannot be directly used in CCM SOCOL, which has no explicit treatment of ion chemistry and requires the conversion of the ionization rates into NO_x and HO_x production rates. The energetic protons in a solar proton event are able to ionize air molecules, $X_2 + p \rightarrow X_2^+ + p + e^*$, producing fast secondary electrons (X = N, O, and the star symbolizes high kinetic energy). These electrons can then dissociate the nitrogen molecule, $N_2 + e^* \rightarrow 2N(^4S; ^2D) + e$, where $N(^4S)$ is the electronic ground state of the nitrogen atom and $N(^2D)$ is its electronic first excited state. Almost all of the $N(^2D)$ atoms react with O_2, producing nitric oxide, $N(^2D) + O_2 \rightarrow$

NO + O (whereas collisional quenching of $N(^2D)$ plays only a minor role). Conversely, the ground state can undergo a 'cannibalistic' reaction with NO, $N(^4S) + NO \rightarrow N_2 + O$, leading to the destruction of NO_x. Therefore, within SOCOL $N(^2D)$ is immediately converted into NO, while $N(^4S)$ is a regular species in the CCM, which is subject to a full kinetic treatment. Following Brasseur and Solomon (2005), when dissociation of molecular nitrogen yields one $N(^4S)$ and one $N(^2D)$ atom, the net odd nitrogen production is extremely small: almost every $N(^2D)$ atom produces one NO molecule, but almost every $N(^4S)$ atom immediately destroys one at these altitudes. Net production is provided only by the very small fraction of $N(^4S)$ atoms which react with oxygen, $N(^4S) + O_2 \rightarrow NO + O$, rather than with NO.

Therefore, a quantification of the $N(^2D)$:$N(^4S)$ branching ratio is required. Following Porter *et al* (1976), 1.25 N molecules are produced per ion pair, of which 55% are $N(^2D)$ and 45% are $N(^4S)$ (see table V in Porter *et al* 1976). In SOCOL, the first excited state, $N(^2D)$, is assumed to convert instantaneously to NO. It is important to note that in the model used here, the ground state atom, $N(^4S)$, may undergo the cannibalistic reaction with the produced NO, i.e. $N(^4S) + NO \rightarrow N_2 + O$, or may react, though much more slowly, with molecular oxygen to generate NO. The production of HO_x has been taken into account using the calculations by Solomon *et al* (1981). They showed that below 60 km altitude about 2 HO_x molecules are produced, dropping towards 1.2 HO_x at 80 km. Egorova *et al* (2011) showed that the NO_x and HO_x parameterizations used in our study compare reasonably well with their model using complete ion chemistry.

In order to simulate the SPE event, we have performed the followed analysis. First we assumed that the event is similar to the Carrington event in 1859 in the fluence of >30 MeV ($F_{30} = 1.9 \times 10^{10}$ cm^{-2}) as estimated by McCracken *et al* (2001). The time profile of injection was taken as proposed by (Shea *et al* 2006, figure 12 therein) with two injections, a smaller one peaked on DOY 240–241 and a major one peaked on DOY 245. Even though the existence of the Carrington SPE is now doubted (Wolff *et al* 2012), we still consider it as the worst case scenario. Then we assume that such a hypothetical event occurred in the year 2020. In order to model the atmospheric effect of such an event we consider two spectral shapes of the SPE energy spectra. A hard spectrum as for the event of February 1956, and a soft spectrum as for the event of August 1972 (see detail in Usoskin *et al* 2011). Then these spectra were scaled to match the SPE fluence proposed for the Carrington-like event. We will regard to these two cases as the hard spectrum (HS) and soft spectrum (SS) scenarios, respectively. These two scenarios were then applied to the 3D CCM SOCOL v2.0. We then carried out three 9-month long runs—a control and two perturbed runs—with ten ensemble members each, starting with atmospheric conditions in August 2020 and ending in April 2021. The ensemble members have been generated by small perturbations (−0.1–+0.1%) of the CO_2 mixing ratio during the first month of the model run. We can compare the Carrington event ionization rates to other SPEs, and as an example we have chosen the October 2003 SPE, which is one of the largest SPEs recorded and for which we have the ionization rates readily available (they have been published, e.g., in Verronen *et al* 2005). We integrated the ionization rates over the duration of the event, so that we can compare the total number of ion pairs produced at each altitude. We find that at 35–60 km the total rates of the Carrington event are 4–4.5 times higher than those of October 2003. This number is similar to the scaling factor used by Thomas *et al* (2007), although they used a different SPE.

3. Results

The ionization rates for the HS and the SS scenarios applied in this study are shown in figure 1, suggesting that the major part of the energy is deposited in the stratosphere (20–40 km in altitude). The characteristics of this solar proton event results in two distinct peaks, with the second peak stronger than the first one at the end of August. We can see that in the upper panel, showing the IR for the HS case, the signal penetrates down to the troposphere whereas the lower panel shows us that the signal hardly reaches down to 10 km.

Figures 3 and 4 as well as 6 and 7 show time series of zonal mean ensemble responses in NO_x, HO_x, ozone and temperature. Figure 5 depicts the response of the HNO_3 flux in the SH averaged over the first month after the event. These results are calculated as a relative deviation of the experimental run for the HS scenario and from the reference run, i.e. the run without the influence of the energetic particles. The results obtained with the ionization rates for the SS scenario derived from Usoskin *et al* (2004) and Usoskin and Kovaltsov (2006) will be discussed later in this chapter when comparing them to the results with IR for the HS scenario.

The results for NO_x (see figure 3) show that the enhancement after this event lasts for weeks after the impact happened, i.e. the changes in odd nitrogen in both hemispheres are visible for about nine weeks. During the solar proton event, a statistical significant increase, computed with the Student T-test, of up to 2000% (∼80 ppbv) is visible in the Northern Hemisphere (NH). In the Southern Hemisphere (SH), the maximum increase of up to 10 000% is shown in the upper troposphere/lower stratosphere (UT/LS) region, whereas an increase of more than 300% (∼70 ppbv) is depicted in an altitude range from 80 down to 60 km. The increase in NO_x and the longevity of the changes are pretty similar when comparing this result with figure 2 in Calisto *et al* (2012), even though in this work, the most intense increase of NO_x in the SH is depicted at the UT/LS region (∼20 km). The reason for that can be explained with figure 2. There we see the peak of ionization in an altitude of about 23 km.

Figure 4 showing the changes in HO_x depict an increase of up to 600% in the NH and an increase of up to 4000% in the SH. This difference is caused by the fact the northern hemisphere has still a higher illumination compared to the southern hemisphere, i.e. the background level of HO_x is larger (Rodger *et al* 2008). The results by Rodger *et al* (2008) are in good agreement when looking at the pattern of the HO_x

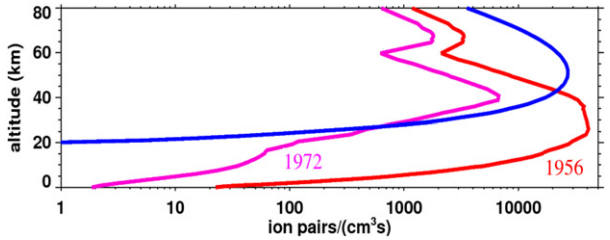

Figure 2. Red and rose lines: ionization rates (ion pairs produced per cm^3 and second) as computed by the CRAC_CRII model (Usoskin *et al* 2010). Blue line: ionization rate used in the papers by Rodger *et al* (2008) and Calisto *et al* (2012).

increase, i.e. the SH shows a more intense enhancement then the NH.

This additional input of NO_x and HO_x, especially in the southern hemisphere, is able to change the HNO_3 deposition fluxes as a response to the Carrington-like event, as we can see in figure 5 which is averaged over the first month after the event. The statistically significant (at better than 95% level) response of up to 50% is simulated in the vicinity of the south pole. The response to this event is less pronounced in the northern hemisphere (not shown). This hemispherical asymmetry is related to the much higher intensity of HNO_3 sources in the NH in comparison with the relatively clean high latitudes in the SH. The model includes dry and wet depositions of O_3, CO, NO, NO_2, HNO_3, and H_2O_2. The dry deposition flux or the removal rates by the absorption of the species at the surface is proportional to the predefined dry deposition velocities which are prescribed for different types of surfaces following Hauglustaine *et al* (1994) and the concentration of the species in the lowest model cell. The dry deposition fluxes of several species from nitrogen group (NO, NO_2, HNO_3 and N_2O_5) are accumulated and stored as monthly mean for all model cells. In addition, the removal of the soluble HNO_3 by tropospheric precipitation is represented by a constant removal rate of 4×10^{-6} s^{-1}. The wet deposition fluxes are not stored.

Losses in ozone of up to 60% and about 40% are visible in the southern and the northern hemisphere, respectively (figure 6). These losses are correlated to the increase in NO_x and HO_x shown in figures 3 and 4 causing a depletion of O_3 from 80 down to about 30 km. Figure 7 depicting the changes in temperature shows a decrease of about 1 K at about 50 km in the northern hemisphere caused by the depletion of ozone which in turn leads to a decrease in solar heating in the sunlit atmosphere. Contrariwise, the southern hemisphere which shows stronger response in the other species, shows no statistical significant cooling. The SPE induced cooling in the polar region increases the pole to equator temperature gradient with repercussion for the zonal winds.

Figure 8 shows the changes in zonal winds averaged from August to November for the NH and the SH at 30 hPa (upper panel) and 50 hPa (lower panel). We see at both altitudes a statistical significant increase of up to 2 ms^{-1} in the northern hemisphere in the polar region. The acceleration of the zonal wind is explained by the fact, that we have a cooling in the upper polar stratosphere due to the ozone depletion in

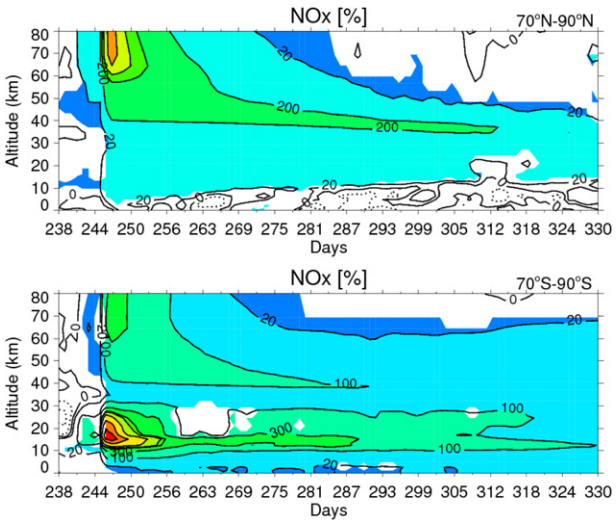

Figure 3. Upper panel shows the changes in NO_x zonal mean mixing ratio profile in the polar region (70–90°N). The lower panel shows the same for 70–90°S. Both panels show the results with the IR from 1956. Colors indicate areas with at least 95% statistical significance. Upper panel contour levels: −20, 0, 20, 200, 700, 1200, 2000, 10 000%. Contour levels lower panel: −20, 0, 20, 100, 300, 800, 1000, 2000, 5000, 10 000%.

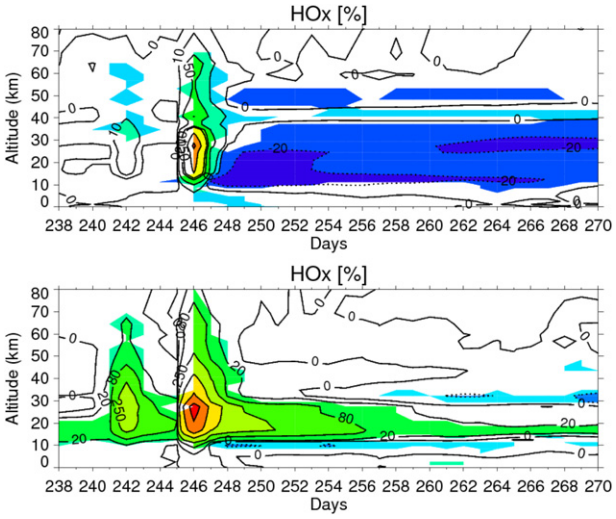

Figure 4. Upper panel shows the changes in HO_x zonal mean mixing ratio profile in the polar region (70–90°N) in per cent. The lower panel shows the same for 70–90°S. Both panels show the results with the IR from 1956. Colors indicate areas with at least 95% statistical significance. Upper panel contour levels: −50, −20, 0, 10, 50, 100, 150, 400, 600%. Contour levels for the lower panel: −50, −20, 0, 20, 80, 250, 800, 2000, 4000%.

this region (see figures 6 and 7), which in turn leads to an acceleration of the zonal wind in agreement with the thermal wind balance (Limpasuvan *et al* 2005). The SH zonal winds seem not to be affected by SPE, we do not have similar effects as we have seen in the northern hemisphere. The reason for that can be explained with figure 7, there we have negligible changes in the temperature due to the solar proton event. Therefore, no changes in the equator–pole temperature gradient.

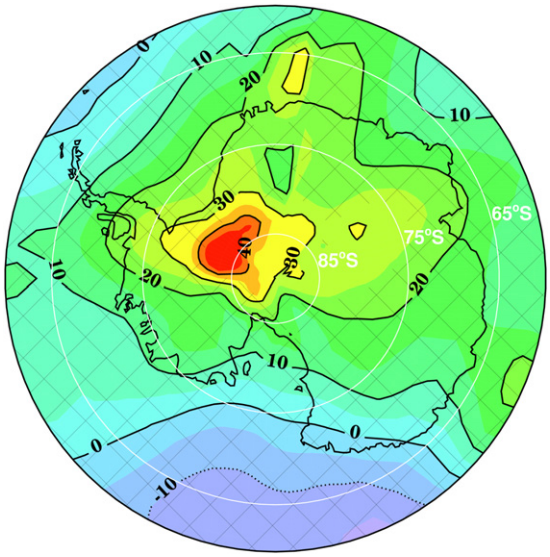

Figure 5. The response of the HNO_3 deposition fluxes (%) in the southern hemisphere averaged over the first month after the event for the 1956 case. Over the stripped area obtained responses are not significant at a 95% confidence level.

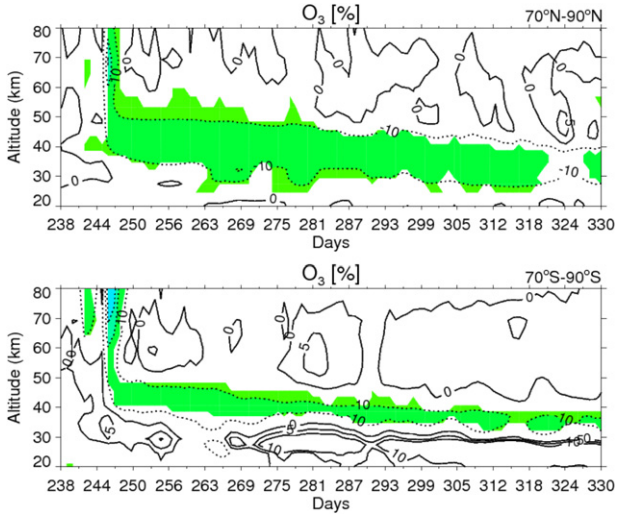

Figure 6. Upper panel shows the changes in ozone zonal mean mixing ratio profile in the polar region (70–90°N) in per cent. The lower panel shows the same for 70–90°S. Both panels show the results with the IR from 1956. Colors indicate areas with at least 95% statistical significance. Contour levels: −80, −60, −40, −10, 0, 5, 10, 50%.

3.1. Comparison of the ionization rates for the hard and the soft spectrum scenarios

As one can see in figures 1 and 2, the ionization rates for the HS and SS scenarios show differences not only in the intensity of ionization but also in how deep the particles penetrate in the atmosphere. It is important to simulate events with different spectra to analyze the difference between them. The importance of how deep the ionization penetrates is visible in figure 9 where the surface air temperature (SAT) is shown. The upper panels represent the SAT for the ionization rates for the HS scenario for January and February, the lower panels

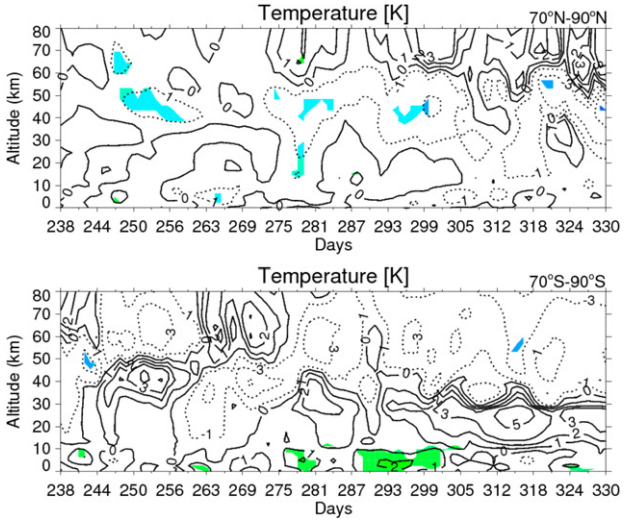

Figure 7. Upper panel shows the changes in zonal mean temperature for the polar region (70–90°N) in Kelvin. The lower panel shows the same for 70–90°S. Both panels show the results with the IR from 1956. Colors indicate areas with at least 95% statistical significance. Contour levels: −6, −3, −1, 0, 1, 2, 3, 5, 10 K.

show the same for the IR for the SS case. This figure reveals, that for January, the ionization for the HS case has a statistical significant warming of up to 7 K over Europe and Russia whereas the ionization for the SS scenario shows neither a statistical significant increase nor a decrease over the above mentioned area. The southern hemisphere, however, shows for both ionization scenarios a negligible decrease north of Antarctica in January. The right side of the panel, showing February, shows still a significant increase over Russia for the IR for the HS whereas the ionization rate for the SS scenario has no statistical significant area over this part of the northern hemisphere. The southern hemisphere still shows just a negligible decrease for the soft spectrum ionization rate.

The general pattern for both ionization rates are in a comparable manner, i.e. they both show a warming over Europa, Russia and the northern part of America in January and February but the intensities and the significance are not the same. Additionally, we see that the effects of the Carrington-like event result in an alternating cooling/warming pattern resembling the typical response of the SAT caused by the intensification of the polar vortex known as the positive phase of Arctic oscillation (Thompson and Wallace 1998), termed AO^+.

Finally, we investigate the influence of such a major solar proton event on the total ozone (TOTOZ) for January and February for both parameterization. The effects on TOTOZ for both hemispheres are displayed in figure 10. The upper panel shows the total ozone, given in DU, for the HS case ionization for January and February whereas the lower panel shows the same for the SS scenario IR. We can see that the upper part of this figure depicts a statistical significant decrease of more than 20 DU over Europe and Russia and a significant increase of up to 30 DU over Canada. Other small decreases are visible but with a lower intensity. Interestingly,

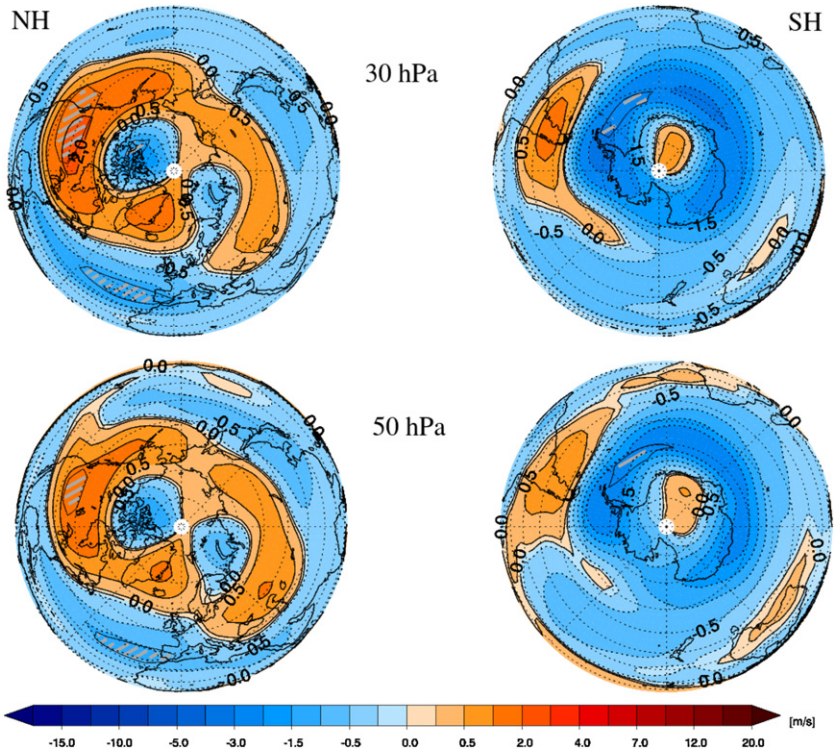

Figure 8. Upper row: polar stereographic projection of zonal wind changes at 30 hPa from August to November given in ms^{-1}. Lower row: zonal wind changes at 50 hPa from August to November given in ms^{-1}. Left column: NH. Right column: SH. Hatched areas show 95% statistical significance.

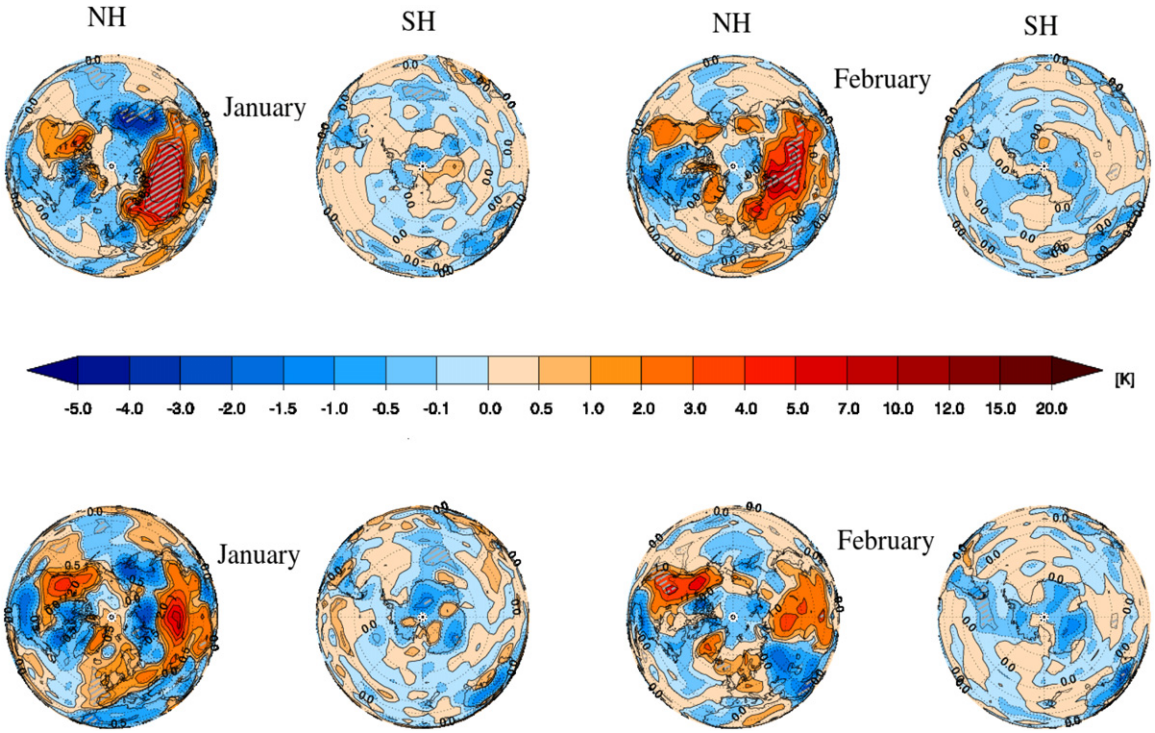

Figure 9. Effect of solar proton event on SAT, [SAT]experimental-[SAT]reference, given in Kelvin for monthly mean. Upper panels: using the ionization rate from 1956 for January (left) and February (right). Lower panels: using the ionization rate from 1972 for January (left) and February (right). Hatched areas indicate changes with at least 95% statistical significance.

the lower part of the figure, showing the IR for the SS case, shows just a small area of significant decrease over Europe and no significant increase over Canada, even though having a larger area of increase. Both ionization show a small, i.e. up to 12 DU increase over Antarctica. When analyzing February, we can see that there is still a decrease of up to 20 DU

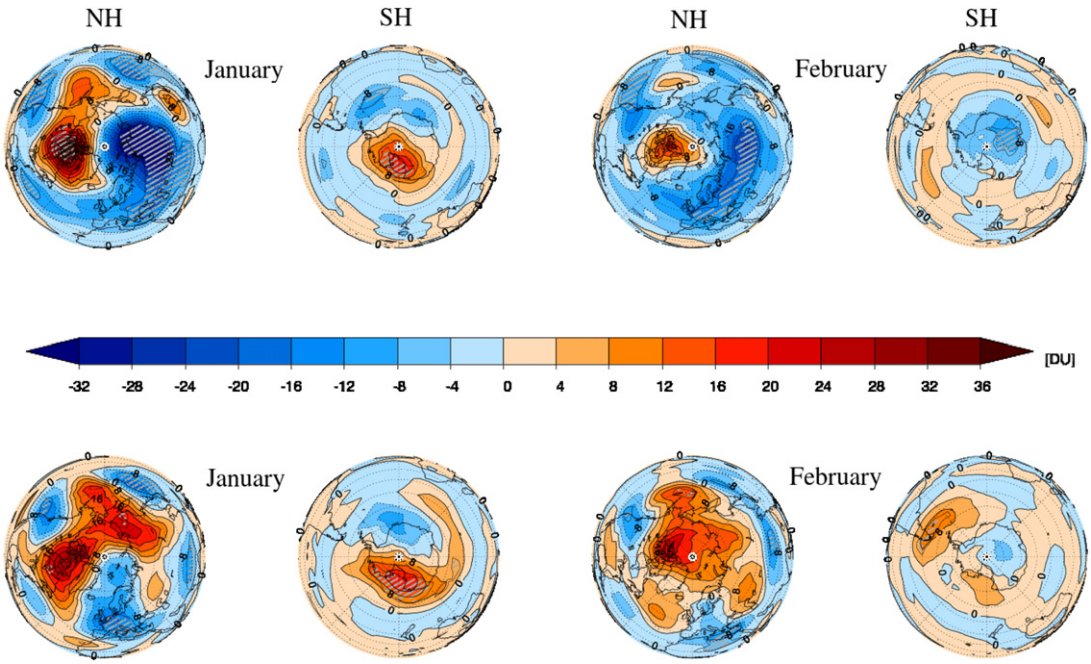

Figure 10. Effect of solar proton event on TOTOZ, [TOTOZ]experimental-[TOTOZ]reference, given in DU for monthly mean. Upper panels: using the ionization rate from 1956 for January (left) and February (right). Lower panels: using the ionization rate from 1972 for January (left) and February (right). Hatched areas indicate changes with at least 95% statistical significance.

visible over Europe and Russia but the area is not as big as in the January plot. The lower plot, showing the IR for the SS case for February shows small areas of decrease with a maximum of 8 DU. These ozone changes are not predicted to occur during the time when the event is happening; rather, the transport of the enhanced odd nitrogen to lower altitudes and therefore higher ozone amounts allows a more substantial total ozone impact. When the polar vortex breaks up, air from lower latitudes which has been less affected by NO_x/HO_x perturbations and ozone depletion enters the region, therefore giving a positive signal in the plot.

The SH, however, shows a different pattern, i.e. the upper part of figure 10 shows a small significant decrease over Antarctica whereas the lower part of this figure shows a small increase at the southernmost part of South America.

For this species, the general pattern between the two ionization rates is not as good as we have seen in figure 8, only in the southern hemisphere in January similar intensities are visible.

These two different ionization rates compared in figures 8 and 9 are similar to the comparison done in the letter by Calisto *et al* (2011) where they analyze the different parameterization for GCR ionization. One of the GCR parameterization stops at 18 km whereas the other one is extended to the surface, similar to figure 1 in this letter, the ionization for the HS case goes down to the surface whereas the one for the SS case shows no direct ionization below about 15 km. Comparing now figure 9 of Calisto *et al* (2011) and figure 9 in this letter, we can see that they show a warming over Europe and Russia and a not significant cooling over Greenland and the eastern part of Canada.

4. Discussion and conclusion

This letter presents a study based on the 3D CCM SOCOL v2.0 of the impact of a major solar proton event. The simulation is made for a worst case event similar to the proposed Carrington event of 1859, assuming a hard (as for the SPE of February 1956) and soft (as for the SPE of August 1972) spectrum of SPEs. The ionization rates have been calculated by Usoskin *et al* (2011) analyzing the effects on atmospheric chemistry, temperature and dynamics from the surface up to the mesopause or approximately 80 km. Here we consider, for the first time for such a study, the full effect of energetic particles in the atmosphere, also in the troposphere and considering also the background variability of galactic cosmic rays that was typically neglected previously.

Our calculations presented in section 3 show the following. The influence of both ionization consist of an increase of NO_x and HO_x and a subsequent increase in HNO_3 as well as a decrease in ozone in the polar mesosphere and the stratosphere, cooling in the polar upper stratosphere with a resulting acceleration of the zonal winds and changes in the surface air temperature and total ozone. Except the temperature (see figure 7) in the southern hemisphere, changes due to the solar proton event are most pronounced shortly after the event happened.

The impact pattern of NO_x, HO_x and ozone modeled in this letter is in good agreement with the results of Calisto *et al* (2012). Our results show for NO_x a long lived change, especially in the northern hemisphere i.e. the increase is visible for several weeks. The same is true for HO_x. We can clearly identify two statistically significant impacts for the SH and for the NH. Interestingly, in this letter, the increase in odd

hydrogen is longer visible than in Calisto *et al* (2012). The reason for this might be that the most intense ionization (see figures 1 and 2) is lower than in Calisto *et al* (2012) which means that the photochemical lifetime of the additional HO_x is longer in the lower altitudes than in higher altitudes. The change in ozone, however, looks similar when looking at the pattern, even though the impact seen in figure 6 is less intense then presented in Calisto *et al* (2012). The reason for this might again be that the most intense increase of the ozone depleting substances, i.e. NO_x and HO_x take place at different altitudes.

The modeled outcome for TOTOZ compared with results of Thomas *et al* (2007) is in reasonable agreement. Thomas *et al* (2007) show in their figures 6 and 7 that the impact of the solar protons on column O_3 is still visible for weeks and months after the event started, similar to our results which show that significant changes are depicted long after the SPE has ended.

The qualitative agreement of the results presented in this letter with those of Thomas *et al* (2007), Calisto *et al* (2011, 2012) strengthen the statement that solar protons do have a statistically significant impact on atmospheric chemistry and dynamics in a broad altitude range going from the troposphere up to the mesosphere with repercussions for the surface air temperature.

Acknowledgments

The authors want to acknowledge to the ISSI teams for stimulating discussions. ER is partially supported by the Swiss National Science Foundation under grant CRSI122-130642 (FUPSOL). IU and ER acknowledge fruitful collaboration inside COST ES1005 TOSCA (www.tosca-cost.eu) team.

References

Barnard L, Lockwood M, Hapgood M A, Owens M J, Davis C J and Steinhilber F 2011 Predicting space climate change *Geophys. Res. Lett.* **38** L16103

Bazilevskaya G A *et al* 2008 Cosmic ray induced ion production in the atmosphere *Space Sci. Rev.* **137** 149–73

Belov A V, Eroshenko E A, Oleneva V A, Struminsky A B and Yanke V G 2001 What determines the magnitude of forbush decreases? *Adv. Space Res.* **27** 625–30

Brasseur G P and Solomon S 2005 *Aeronomy of the Middle Atmosphere* 3rd edn (Dordrecht: Springer)

Calisto M, Usoskin I, Rozanov E and Peter T 2011 Influence of Galactic Cosmic Rays on atmospheric composition and dynamics *Atmos. Chem. Phys.* **11** 4547–56

Calisto M, Verronen P T, Rozanov E and Peter T 2012 Influence of a Carrington-like event on the atmospheric chemistry, temperature and dynamics *Atmos. Chem. Phys.* **12** 1–8

Egorova T, Rozanov E, Ozolin Y, Shapiro A, Calisto M, Peter T and Schmutz W 2011 The atmospheric effects of October 2003 solar proton event simulated with the chemistry-climate model SOCOL using complete and parameterized ion chemistry *J. Atmos. Sol.-Terr. Phys.* **73** 356–65

Egorova T, Rozanov E, Zubov V and Karol I L 2003 Model for investigating ozone trends (MEZON) *Izv. Atmos. Ocean. Phys.* **39** 277–92

Egorova T, Rozanov E, Zubov V, Manzini E, Schmutz W and Peter T 2005 Chemistry-climate model SOCOL: a validation of the present-day climatology *Atmos. Chem. Phys.* **5** 1557–76

Hauglustaine D A, Granier C, Brasseur G and Megie G 1994 The importance of atmospheric chemistry in the calculation of radiative forcing on the climate system *J. Geophys. Res.* **99** 1173–86

Humble J E 2006 The solar events of August/September 1859—surviving Australian observations *Adv. Space Res.* **38** 155–8

Jackman C H, Marsh D R, Vitt F M, Garcia R R, Randall C E, Fleming E L and Frith S M 2009 Long-term middle atmospheric influence of very large solar proton events *J. Geophys. Res.* **114** D11304

Kane R P 2010 Severe geomagnetic storms and forbush decreases: interplanetary relationships reexamined *Ann. Geophys.* **28** 479–89

Limpasuvan V, Hartmann D L, Thompson D L H, Jeev K and Yung Y L 2005 Stratosphere–troposphere evolution during polar vortex intensification *J. Geophys. Res.* **110** D24101

Manzini E, McFarlane N A and McLandress C 1997 Impact of the Doppler spread parameterization on the simulation of the middle atmosphere circulation using the MA/ECHAM4 general circulation model *J. Geophys. Res. Atmos.* **102** 25751–62

McCracken K G, Dreschhoff G A M, Zeller E J, Smart D F and Shea M A 2001 Solar cosmic ray events for the period 1561–1994 1. Identification in polar ice, 1561–1950 *J. Geophys. Res.* **106** 21585–98

Patterson J D, Armstrong T P, Laird C M, Detrick D L and Weatherwax A T 2001 Correlation of solar energtic protons and polar cap absorption *J. Geophys. Res.* **106** 149–63

Porter H S, Jackman C H and Green A E S 1976 Efficiencies for production of atomic nitrogen and oxygen by relativistic proton impact in air *J. Chem. Phys.* **65** 154–67

Randall C E, Siskind D E and Bevilacqua R M 2001 Stratospheric NO_x enhancements in the southern hemisphere vortex in winter/spring of 2000 *Geophys. Res. Lett.* **28** 2385–8

Reames D V 1999 Particle acceleration at the Sun and in the heliosphere *Space Sci. Rev.* **90** 413–91

Reid G C, Solomon S and Garcia R R 1991 Response of the middle atmosphere to the solar proton events of August–December 1989 *Geophys. Res. Lett.* **18** 1019–22

Rodger C J, Verronen P T, Clilverd M A, Seppälä A and Turunen E 2008 Atmospheric impact of the Carrington event solar protons *J. Geophys. Res.* **113** D23302

Rozanov E, Schlesinger M E, Zubov V, Yang F and Andronova N G 1999 The UIUC three-dimensional stratospheric chemical transport model: description and evaluation of the simulated source gases and ozone *J. Geophys. Res.* **104** 755–81 11

Schraner M *et al* 2008 Chemistry climate model SOCOL: version 2.0 with improved transport and chemistry/microphysics schemes *Atmos. Chem. Phys.* **8** 5957–74

Seppälä A, Verronen P T, Kyrölä E, Hassinen S, Backman L, Hauchecorne A, Bertaux J L and Fussen D 2004 Solar proton event of October–November 2003: ozone depletion in the northern hemisphere polar winter seen by GOMOS/Envisat *Geophys. Res. Lett.* **31** L19107

Shea M A, Smart D F, McCracken K G, Dreschhoff G A M and Spence H E 2006 Solar proton events for 450 years: the Carrington event in perspective *Adv. Space Res.* **38** 232–8

Solomon S, Reid G C, Rusch D W and Thomas R J 1983 Mesospheric ozone depletion during the solar proton event of July 13, 1982. 2. Comparison between theory and measurements *Geophys. Res. Lett.* **10** 257–60

Solomon S, Rusch D W, Gerard J-C, Reidt G C and Crutzen P J 1981 The effect of particle precipitation events on the neutral

and ion chemistry of the middle atmosphere: II. Odd hydrogen *Planet. Space Sci.* **29** 885–92

Thomas B C, Jackman C H and Melott A L 2007 Modeling atmospheric effects of the September 1859 solar flare *Geophys. Res. Lett.* **34** L06810

Thompson D W J and Wallace J M 1998 The Arctic oscillation signature in the wintertime geopotential height and temperature fields *Geophys. Res. Lett.* **25** 1297–300

Tsurutani B T, Gonzalez W D, Lakhina G S and Alex S 2003 The extreme magnetic storm of 1–2 September 1859 *J. Geophys. Res.* **108** 1268

Usoskin I G, Braun I, Gladysheva O G, Hörandel J R, Jämsen T, Kovaltsov G A and Starodubtsev S A 2008 Forbush decreases of cosmic rays: energy dependence of the recovery phase *J. Geophys. Res.* **113** A07102

Usoskin I G, Desorgher L, Velinov P, Storini M, Flückiger E O, Bütikofer R and Kovaltsov G A 2009 Ionization of the Earth's atmosphere by solar galactic cosmic rays *Acta Geophys.* **57** 88–101

Usoskin I G, Gladysheva O G and Kovaltsov G A 2004 Cosmic ray incudec ionization in the atmosphere: spatial and temporal changes *J. Atmos. Sol.-Terr. Phys.* **66** 1791–6

Usoskin I G and Kovaltsov G A 2006 Cosmic ray induced ionization in the atmosphere: full modeling and practical applications *J. Geophys. Res.* **111** D21206

Usoskin I G, Kovaltsov G A and Mironova I A 2010 Cosmic ray induced ionization model CRAC:CRII: an extension to the upper atmosphere *J. Geophys. Res.* **115** D10302

Usoskin I G, Kovaltsov G A, Mironova I A, Tylka A J and Dietrich W F 2011 Ionization effect of solar particle GLE events in low and middle atmosphere *Atmos. Chem. Phys.* **11** 1979–88

Verronen P T, Seppälä A, Clilverd M A, Rodger C J, Kyrölä E, Enell C F, Ulich T and Turunen E 2005 Diurnal variation of ozone depleting during the October–November 2003 solar proton events *J. Geophys. Res.* **110** A09S32

von Clarmann T, Funke B, Lopez-Puertas M, Kellmann S, Linden A, Stiller G P, Jackman C H and Harvey V L 2013 The solar proton events in 2012 as observed by MIPAS *Geophys. Res. Lett.* **40** 2339–43

Wolff E W, Bigler M, Curran M A J, Dibb J E, Frey M M, Legrand M and McConnell J R 2012 The Carrington event not observed in most ice core nitrate records *Geophys. Res. Lett.* **39** L08503